HAL
open science

Irradiance Dependence of the Short-Circuit Current Temperature Coefficient of sc-Si PV Module

Baojie Li, Anne Migan-Dubois, Claude Delpha, Demba Diallo

To cite this version:

Baojie Li, Anne Migan-Dubois, Claude Delpha, Demba Diallo. Irradiance Dependence of the Short-Circuit Current Temperature Coefficient of sc-Si PV Module. IEEE Photovoltaic Specialists Conference (PVSC 2020), Jun 2020, Calgari (virtual), Canada. 10.1109/PVSC45281.2020.9300416 . hal-02903351

HAL Id: hal-02903351

https://centralesupelec.hal.science/hal-02903351

Submitted on 4 Nov 2021

HAL is a multi-disciplinary open access archive for the deposit and dissemination of scientific research documents, whether they are published or not. The documents may come from teaching and research institutions in France or abroad, or from public or private research centers.

L'archive ouverte pluridisciplinaire **HAL**, est destinée au dépôt et à la diffusion de documents scientifiques de niveau recherche, publiés ou non, émanant des établissements d'enseignement et de recherche français ou étrangers, des laboratoires publics ou privés.

Irradiance Dependence of the Short-Circuit Current Temperature Coefficient of sc-Si PV Module

Baojie LI
GeePs - Université Paris-Saclay, CentraleSupélec, CNRS
L2S - Université Paris-Saclay, CNRS, CentraleSupélec
Gif-sur-Yvette, France
baojie.li@centralesupelec.fr

Anne MIGAN-DUBOIS
GeePs - Université Paris-Saclay, CentraleSupélec, CNRS
Gif-sur-Yvette, France
anne.migan-dubois@geeps.centralesupelec.fr

Claude DELPHA
L2S - Université Paris-Saclay, CNRS, CentraleSupélec
Gif-sur-Yvette, France
claude.delpha@centralesupelec.fr

Demba DIALLO
GeePs - Université Paris-Saclay, CentraleSupélec, CNRS
Gif-sur-Yvette, France
demba.diallo@ centralesupelec.fr

***Abstract*— Temperature coefficient of short-circuit current ($TC_{I_{sc}}$) of PV modules plays an important role in PV modeling and I-V characteristic correction. Many standards and researches have indicated that $TC_{I_{sc}}$ is irradiance-dependent, but the detailed relationship is not really clarified. Thus, this paper investigates the relationship of module $TC_{I_{sc}}$ with irradiance from both indoor and outdoor tests and reveal the impact of the varying $TC_{I_{sc}}$ in common applications.**

Keywords— Photovoltaics, temperature coefficient, short-circuit current, current correction, sc-Si module

I. INTRODUCTION

Temperature coefficient of short-circuit current ($TC_{I_{SC}}$) of photovoltaic (PV) module is a crucial parameter for PV system [1]. It is widely used for PV modeling [2] and the correction of field-measured current data [3], e.g., the current at maximum power point (I_{mpp}) or the current of I-V curve. The application in current correction, specifically, is also an important step for various subsequent performance and reliability analysis, such as PV degradation assessment [4], PV fault detection and diagnosis [5] .

Generally, $TC_{I_{SC}}$ is provided in the manufacture datasheet but always for Standard Test Condition (STC, module temperature T_m=25°C, in-plane irradiance G=1000W/m^2, air mass AM=1.5). However, many standards like [3,6] have pointed out that the value of $TC_{I_{SC}}$ is only valid within a certain range of irradiance. Nevertheless, there is little research dedicated to explain how the module $TC_{I_{SC}}$ varies with G. In the literature, Muhammad et al. [7] observed a decreasing trend of $TC_{I_{SC}}$ with G, but the research is limited to cell level. Manoj et al. [8] focused on the module level $TC_{I_{SC}}$ and captured similar trend, but the precision is hindered as there are only 4 observations measured at different T_m for each G, which are inadequate to fully exhibit the relationship of I_{SC} with T_m and to extract reliable $TC_{I_{SC}}$ values.

Since the dependence of $TC_{I_{SC}}$ on G is not always clear, therefore, in most cases, it is considered as a constant value for convenience [4,5]. However, the impact of this assumption is rarely specified. Consequently, this paper is conceived to evaluate the relationship of module $TC_{I_{SC}}$ with G by both indoor and outdoor tests and then discuss the impact of the varying $TC_{I_{SC}}$ in its common applications.

II. METHODOLOGY OF $TC_{I_{SC}}$ CALCULATION

According to IEC 60891 [3], the calculation of module $TC_{I_{SC}}$ can be summarized in the following steps:

- Step 1: Collect module I_{SC} measured at same G level but with different T_m;
- Step 2: Plot I_{SC} as a function of T_m, fit the whole curve linearly with a least-squares function;
- Step 3: Record the slope of the fitted line as the absolute $TC_{I_{SC}}$ (expressed in A/°C), while the relative (expressed in %/°C) could be determined by dividing the absolute coefficient with the I_{SC} value at STC.

In this calculation procedure, Step 1 is relatively difficult because of its two simultaneous constraints on G and T_m.

Besides, a continuous variation of T_m in a wide range (≥30°C) is also suggested in [3]. Some test schemes can be adopted to collect the required I_{SC}. Using solar simulator and T_m control device is one choice, which permits to perform superior spectrum match. However, the expense of this test is also high, especially when dealing with PV samples of large size, e.g., PV module sample instead of cell sample. Consequently, two cost efficient test procedures are proposed in the followings and adopted in our research to collect the required I_{SC} for the study of $TC_{I_{SC}}$.

- Procedure 1: Collect data in indoor controlled irradiance condition (e.g., using Xenon or Halogen lamps)
- Procedure 2: Collect data under natural sunlight in a short time (assuming G varies very little in this interval)

The details and the experimental setup of these two test procedures will be presented in the next section.

III. Experimental Setup

A. Basic experimental test bench

A MX-50Wp sc-Si module is considered for both indoor and outdoor tests with the datasheet parameters shown in TABLE I.

TABLE I. Parameters of tested sc-Si module

Parameters	Value	Parameters	Value
V_{OC}	21.9V	I_{SC}	2.97A
V_{MP}	18.6V	V_{MP}	2.68A
Relative $TC_{V_{OC}}$	0.28%/°C	Relative $TC_{I_{SC}}$	0.074%/°C

A reference cell (RG100) measures the plane-of array irradiance (G_{POA}) and a Pt100 probe (class A) measures the back-sheet T_m. The module I_{SC} is measured with a programmed source meter (Keithley 2440).

B. Indoor test under controlled irradiance

The test setup is shown in Fig. 1, where 4 halogen lamps provide illumination (non-uniformity $< 10\%$) to the tested module. G could be adjusted continuously from 0 to 1400 W/m^2 by controlling the lamp current. The specific test procedure contains the following steps:

- Step 1: Cool down the test module by using an electric fan with the lamps turned off until the backsheet T_m stabilizes to room temperature.
- Step 2: Adjust G, let the module warm up by the effect of illumination until the backsheet T_m reaches stable operating temperature. During the process, record G_{POA}, T_m and I_{SC} every 2 seconds.
- Step 3: Repeat Step 1-2 with different G values.

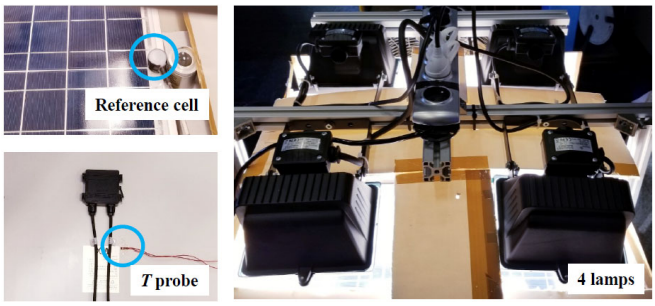

Fig. 1. Experimental setup of indoor controlled -irradiance test

C. Outdoor short-time test under natural sunlight

Outdoor test has a similar test procedure:

- Step 1: Cool the module with a fan in shaded place until T_m stabilized to ambient temperature.
- Step 2: In cloudless weather, move the module (with measurement devices together installed on a movable trolley as shown in Fig. 2) to sunlit place.
- Step 3: Let the module naturally warm up in short time (minimize the impact of changing G) with T_m approaching operating temperature. During the process, record G_{POA}, T_m and I_{SC} every 2 seconds.
- Step 4: Repeat Step 1-3 for different time slots in the same day for different G levels.

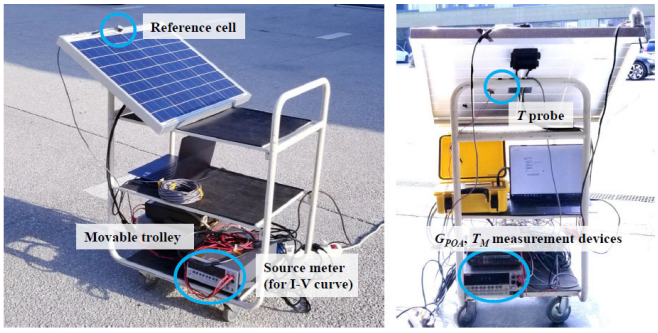

Fig. 2. Experimental setup of outdoor short-time test

IV. Results and Analysis

A. Correction of I_{SC} based on measured G_{POA}

In fact, based on our measurement results, G is not stable for both indoor and outdoor tests, i.e., indoor G_{POA} varies by $\pm 3\%$, due to voltage fluctuation while outdoor G_{POA} varies by $\pm 4\%$, due to the change of sun position). Thus, it is necessary to correct the I_{SC} measured under variable G to a value (I_{SC}^c) under same G (here, G at STC) via the following equation [3]:

$$I_{SC}^c = I_{SC} \cdot G_{STC}/G \tag{1}$$

After the correction, $TC_{I_{SC}}$ could then be calculated based on the procedure presented in Section II.

B. Indoor test results

Several indoor tests were performed with a G_{POA} covering a range from 300 to 1100 W/m^2. One test result with an average

G_{POA} at 883 W/m^2 is presented in Fig. 3 to illustrate the calculation of $TC_{I_{SC}}$.

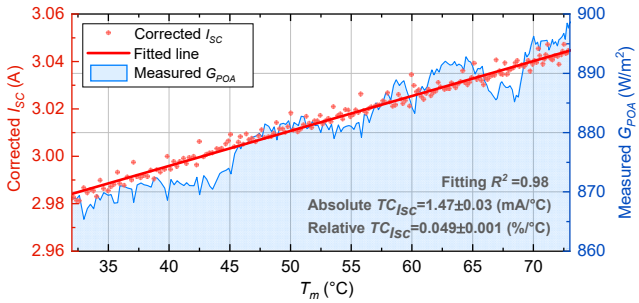

Fig. 3. Indoor test result with average G_{POA} at 883 W/m^2

As illustrated in Fig. 3, the corrected I_{SC} exhibits a linear relationship with T_m during the test period (T_m varies from 32 to 73°C). After linear fitting via Matlab (fitting R^2=0.98), the absolute and the relative $TC_{I_{SC}}$ (dividing the absolute value by I_{SC} at STC from datasheet) are obtained as 1.47 mA/°C and 0.049 %/°C, respectively. In this manner, the relative $TC_{I_{SC}}$ of all the tests can be obtained .The results are presented in Fig. 4 the corresponding variation of T_m also illustrated.

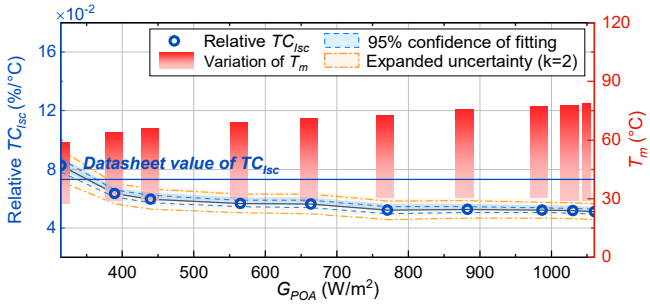

Fig. 4. Indoor test results under different irradiance levels

It is observed from that Fig. 4, firstly, for each test, the T_m of tested module, via warming up by the effect of illumination, spreads a wide range of variation. The difference between inital and final T_m could reach or exceed 30 °C, especially for the test at high G_{POA}. This wide range of variation permits to fully examine the linear relationship of I_{SC} with T_m and extract the $TC_{I_{SC}}$ with more precision.

As for the behavior of $TC_{I_{SC}}$, the relative $TC_{I_{SC}}$ shows a decreasing trend with G_{POA} and the decline rate slows down as G_{POA} increases. Therefore, $TC_{I_{SC}}$ at high G_{POA} (G_{POA} > 700 W/m^2) is relatively stable, but the value is inferior to the datasheet value with the relative error up to 31.1%.

C. Outdoor test results

From 8 am to 12 am on 2019/09/03, several outdoor tests were performed. Taking one test result (shown in Fig. 5) as example, a linear evolution of corrected I_{SC} with T_m is also observed but with larger fluctuations (fitting R^2=0.78) than the indoor test result. This may be due to the more variable environmental conditions (e.g., impact of wind).

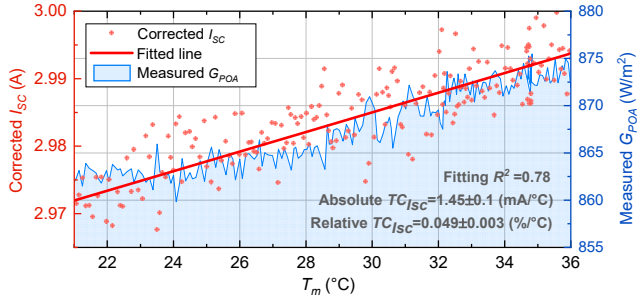

Fig. 5. Outdoor test result with average G_{POA} at 868 W/m^2

Similarly, the calculated $TC_{I_{SC}}$ at different sunlight are plotted in Fig. 6. From the results, firstly, it is observed that the variation of T_m increases gradually with G_{POA} and but is relatively lower than that for indoor test. This is mainly due to the fact that outdoor tests are carried on in open space (where ambient temperature is relatively stable during each short-time test) rather than the confined space of indoor tests (where the ambient temperature also increases), so the variation of T_m is not that significant.

Regarding the $TC_{I_{SC}}$, a similar decreasing trend of $TC_{I_{SC}}$ with G_{POA} is also found. There are certain parts not perfectly matching with the indoor test results, like the $TC_{I_{SC}}$at low G_{POA} range, where larger values are observed. Nevertheless, the general variation tendency is coherent with that of indoor test results, like decreasing decline rate with G_{POA} and the relatively stabilized value at high G_{POA} range. In this stabilized range, the value of $TC_{I_{SC}}$ is found also coherent, which are around 0.05%/°C.

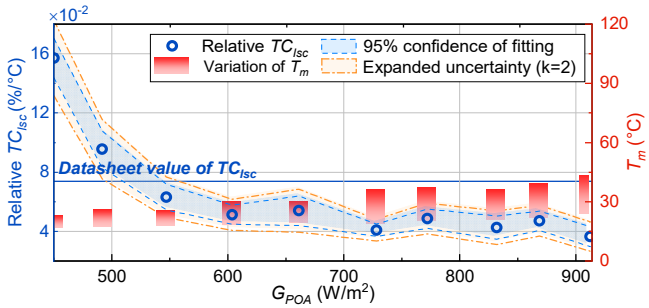

Fig. 6. Outdoor test results under sunlight irradiance levels

D. Effect of a Variable $TC_{I_{SC}}$

From indoor and outdoor tests, the calculated $TC_{I_{SC}}$ shows significant variation particularly with the G_{POA} at low values (<400 W/m^2). In order to evaluate the impact of this variation, let's consider the application in current correction using (2) as an example.

$$I_2 = I_1 \cdot \left(1 + TC_{I_{SC}} \cdot (T_2 - T_1)\right) \cdot G_2/G_1 \qquad (2)$$

where, I_1 and I_2 are the current before and after correction; G_1 and G_2, T_1 and T_2 are the measured and desired irradiance or module temperature, respectively.

Assuming that I_1 is the measured current at low irradiance G_1 (e.g., 400 W/m^2) and the measured $TC_{I_{SC}}$ at G_1 is 0.16%/°C (according to Fig. 6). When $(T_2 - T_1)$ drops in the range [20°C,50°C], and if the datasheet value of $TC_{I_{SC}}$ (0.07%/°C) is used to correct I_1, the relative error of I_2, compared to the result using the real measured $TC_{I_{SC}}$, lies between 1.7-4.2%. If using $TC_{I_{SC}}$ at high G_{POA} (e.g., 0.05%/°C), the error will reach 2.1-5.1%. These errors can hinder the realization of high-precision current correction and degrade the current-based module performance analysis.

V. Uncertainty analysis

The uncertainty characterizes the range of values within which the true value of one measurand is considered to lie with certain level of confidence [9]. The uncertainty involved in the calculation of $TC_{I_{SC}}$ is determined by the uncertainty of 3 measurands, i.e., G_{POA}, T_m and I_{SC}. For each measurand, the uncertainty addresses the measurement error from 2 effects, the random effect caused by the stochastic variation of measurement device and the systematic effect caused by persistent issue which leads to a consistent error [10]. For G_{POA}, the systematic effect mainly results from the spectral mismatch of reference cell, the alignment of sensor with tested module [11], etc.; For T_m, the systematic effect is mainly caused by the calibration, uniformity of backsheet T_m and the difference between the rear side T_m and the cell temperature [11]. Using infrared (IR) camera, the distribution of module T_m is available to examine. Two examples taken during the outdoor tests are shown in Fig. 7. It is observed a clear nonuniform distribution of T_m, which is commonly encountered due to the wind and physical irregularities (like module frame and junction box) [12]. The maximum variation of rear side T_m is within 3°C, which meets the requirement proposed in [3] for the correction analysis.

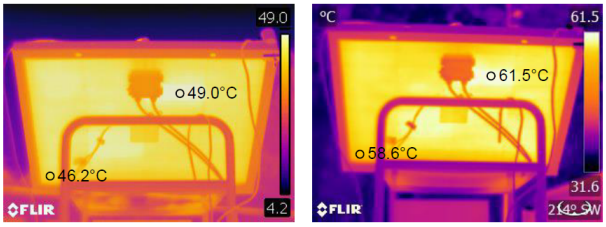

Fig. 7. IR images of module backside during outdoor tests

In order to quantify the impact of these uncertainty on $TC_{I_{SC}}$, the uncertainty propagation analysis is performed. Firstly, since relative $TC_{I_{SC}}$ is calculated by the slope of I_{SC}^c with T_m (by linear fitting) normalized by I_{SC}^{STC}, a simplified function, which is based on the difference of T_m (ΔT_m) and I_{SC}^c (ΔI_{SC}^c) between 2 observations (with similar G but considerably different T_m), is used to present the calculation of the relative $TC_{I_{SC}}$ as:

$$TC_{I_{SC}} = \frac{1}{I_{SC}^{STC}} \cdot \frac{\Delta I_{SC}^c}{\Delta T_m} \tag{3}$$

Then, replace the ΔI_{SC}^c by the difference of the corresponding measured I_{SC} (ΔI_{SC}) via (1) (supposing the G of the 2 observations are identical):

$$TC_{I_{SC}} = \frac{1}{I_{SC}^{STC}} \cdot \frac{\Delta I_{SC} \cdot \frac{G_{STC}}{G}}{\Delta T_m} = \frac{G_{STC}}{I_{SC}^{STC}} \cdot \frac{\Delta I_{SC}}{\Delta T_m G} \tag{4}$$

In this manner, the relation of relative $TC_{I_{SC}}$ with the measured parameters, $TC_{I_{SC}}$=$f(G, \Delta I_{SC}, \Delta T_m)$, is available for uncertainty analysis. Here, we consider the relative standard uncertainty (u^r), which is the absolute uncertainty divided by the best estimate of one measurand [9]. For a function $y = f(X_1, X_2, X_3) = K \cdot X_1/(X_2 X_3)$, where K is a constant and $X_i (i = 1,2,3)$ are the measurands, the propagated u_y^r based on the $u_{X_i}^r (i = 1,2,3)$ could be calculated as [9]:

$$|u_y^r| = \sqrt{\sum_{i=1}^{3} u_{X_i}^{r2} + 2\sum_{i=1}^{2}\sum_{j=i+1}^{3} u_{X_i}^r u_{X_j}^r r(X_i, X_j)} \tag{5}$$

where $r(X_i, X_j)$ represents the correlation coefficient between X_i and X_j.

Based on the datasheet of measurement devices and the reported common measurement systematic uncertainty [11,13], the combined u_G^r, $u_{\Delta I_{SC}}^r$ and $u_{\Delta T}^r$ are considered as 5%, 0.1% and 2% (using a coverage factor $k = 2$), respectively. Here, the u^r of ΔI_{SC} and ΔT_m are set relatively lower than that of G. This is out of the consideration that the parameters (ΔI_{SC} and ΔT_m) used in (4) are the difference values, thus the impact of systematic error (like calibration bias, the difference between rear side T_m and cell T), which is generally larger than the random dispersion, could be reduced.

In fact, all the measurands G, ΔI_{SC} and ΔT_m are correlated but with different r. For example, ΔI_{SC} is quasi linearly correlated with G with $r(G, \Delta I_{SC}) \approx 1$, while ΔT_m, i.e., the variation of the T_m between 2 chosen observations, is nearly uncorrelated with G or ΔI_{SC}. Therefore, for simplification, we consider $r(G, \Delta I_{SC}) = 1$, $r(\Delta T_m, \Delta I_{SC}) = r(\Delta T_m, G) = 0$. In this way, based on (5), the propagated u^r of $TC_{I_{SC}}$ could be expressed as:

$$\left|u_{TC_{I_{SC}}}^r\right| = \sqrt{u_G^{r2} + u_{\Delta I_{SC}}^{r2} + u_{\Delta T}^{r2} + 2 \cdot u_G^r \cdot u_{\Delta I_{SC}}^r} \tag{6}$$

The $u_{TC_{I_{SC}}}^r$ equals 5.5%, which means that the $TC_{I_{SC}}$ will fluctuate by ±5.5% around the calculated value due to the uncertainty of the 3 measurands. Now, we add this uncertainty to the results obtained in previous section and reshow them in Fig. 8 and Fig. 9. From the results, it is observed that the uncertainty introduced by the 3 measurands has no significant impact on the global decreasing trend of the obtained $TC_{I_{SC}}$.

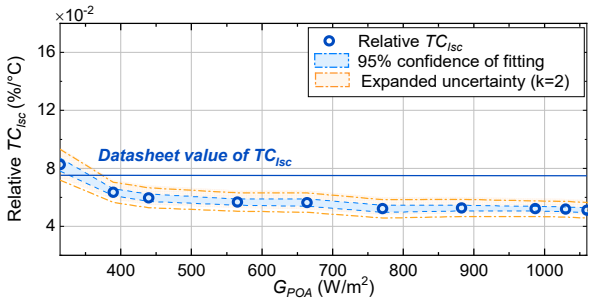

Fig. 8. Indoor test results with uncertainty added

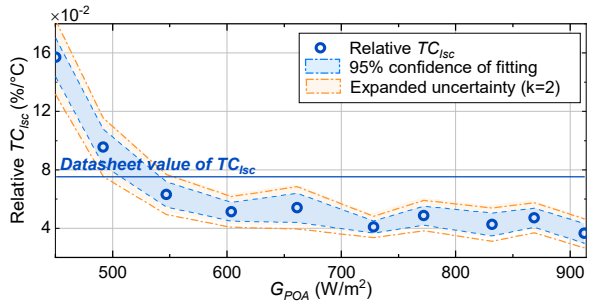

Fig. 9. Outdoor test results with uncertainty added

VI. Discussion

The observed trend in the variation of $TC_{I_{SC}}$ with G is consistent with the reported results at cell level [7] and at module level under solar simulator [8]. Since $TC_{I_{SC}}$ has been validated spectrum-dependent [14], this G-dependent phenomenon may be partially the impact of spectrum. For outdoor test under clear sky, from morning to noon, G increases with time, but the energy portion in near infrared range decreases. Since $TC_{I_{SC}}$ responds significantly to this range of wavelength [15], the change of spectrum could lead to the decrease of $TC_{I_{SC}}$. However, for indoor test, the spectrum is relatively stable. Therefore, this could not fully explain the phenomenon. It clearly requires further exploration.

VII. Conclusion

The dependence of sc-Si module $TC_{I_{SC}}$ on irradiance is investigated in this paper. A decreasing trend is observed from both indoor and outdoor tests. The decline rate slows down as G_{POA} increases. Thus $TC_{I_{SC}}$ at high G_{POA} range is almost constant but to a value lower than the one given in datasheet. We have shown that if an improper value of $TC_{I_{SC}}$ is applied, an error of up to 5% in current correction could be reached. Future research will continue to study the G dependence of $TC_{I_{SC}}$ on other technologies of PV modules (like a-Si, CdTe, HIT), to quantify the impact of several factors (like I_{SC} correction method, installation position of T_m probe) on the test results and to analyze the underlying mechanism of the variation of $TC_{I_{SC}}$.

References

[1] R Dubey, P Batra, S Chattopadhyay, A Kottantharayil, BM Arora, KL Narasimhan, et al. “Measurement of temperature coefficient of photovoltaic modules in field and comparison with laboratory measurements,” in Proceedings of IEEE 42nd Photovoltaic Specialist Conference, New Orleans, LA, USA, 14-17 Jun., 2015, pp. 1–5.

[2] I de la Parra, M Muñoz, E Lorenzo, M García, J Marcos, F Martínez-Moreno. “PV performance modelling: A review in the light of quality assurance for large PV plants,” Renew Sustain Energy Rev, vol. 78, pp. 780–97, 2017.

[3] IEC 60891. “Photovoltaic devices - Procedures for temperature and irradiance corrections to measured I-V characteristics,” IEC, Standard, 2009

[4] J Eduardo, FS De Oliveira, C Wilhelm, M Prieb. “Degradation analysis of a photovoltaic generator after operating for 15 years in southern Brazil,” Sol Energy, vol. 196, no. 2019, pp. 196–206, 2020.

[5] H Zhu, L Lu, J Yao, S Dai, Y Hu. “Fault diagnosis approach for photovoltaic arrays based on unsupervised sample clustering and probabilistic neural network model,” Sol Energy, vol. 176, pp. 395–405, 2018.

[6] IEC 61853-1. “Photovoltaic (PV) module performance testing and energy rating - Part 1: Irradiance and temperature performance measurements and power rating,” IEC, Standard, 2011

[7] T Muhammad, O Jan Ove, S Tor Oskar. “Temperature Coefficients of Solar Cells from Elkem Solar under Varied Intensities and Selective Wavelength Regions of the \textsc{AM} 1.5 Spectrum,” in Proceedings of 29th EU PVSEC 2014, Amsterdam, Netherlands, 22-24 Sep., 2014, pp. 3378–82.

[8] M Morampudi, B Bora, G Kumar, R Kumar, R Siddiqui, S et al. “Performance comparision of PV module based of temperature cofficient in indoor and outdoor conditions as per IEC 61853-1,” in Proceedings of 32nd EU PVSEC 2016, Munich, Germany, 21-24 Jun., 2016, pp. 2067–9.

[9] JCGM. “Evaluation of measurement data-Guide to the expression of uncertainty in measurement Évaluation des données de mesure-Guide pour l’expression de l’incertitude de mesure,” JCGM, Report, 2008

[10] JM Bland, DG Altman. “Statistics notes: Measurement error,” BMJ, vol. 312, no. 7047, pp. 1654–1654, 1996.

[11] C Reise, B Müller, D Moser, G Belluardo, P Ingenhoven. “Report IEA-PVPS T13-12:2018 Uncertainties in PV System Yield Predictions and Assessments,” IEA, Report, 2018

[12] DL King, JA Kratochvil, WE Boyson. “Temperature coefficients for PV modules and arrays: Measurement methods, difficulties, and results,” in Proceedings of the 26th IEEE Photovoltaic Specialists Conference, Anaheim, CA, USA, 29 Sept.-3 Oct., 1997, pp. 1183–6.

[13] D Dirnberger, U Kraling. “Uncertainty in PV module measurement-part i: Calibration of crystalline and thin-film modules,” IEEE J Photovoltaics, vol. 3, no. 3, pp. 1016–26, 2013.

[14] CR Osterwald, M Campanelli, T Moriarty, KA Emery, R Williams. “Temperature-dependent spectral mismatch corrections,” IEEE J Photovoltaics, vol. 5, no. 6, pp. 1692–7, 2015.

[15] K Ramspeck, F Plag, F Haas, S Winter, A Metz. “Temperature Coefficients of Silicon Solar Cells,” in Proceedings of 31st EU PVSEC 2015, Hamburg, Germany, 14-18 Sep., 2015, pp. 799–803.